The current issue and full text archive of this journal is available at
http://www.emerald-library.com/ft

Rewetting of an infinite tube with internal heating

A.K. Satapathy and R.K. Sahoo
Mechanical Engineering Department, Regional Engineering College, Rourkela, Orissa, India

Received June 2000
Accepted December 2000

Keywords *Quenching, Heat flux, Finite differences*

Abstract *A numerical study has been made to investigate the effect of internal heating and precursory cooling during quenching of an infinite tube. The finite difference solution gives the quench front temperature as a function of various model parameters such as Peclet number, Biot number and dimensionless heat flux. The parametric dependence of the rewetting rate is obtained by the condition that the surface can only be wetted when its temperature is below the quench front temperature. Also, the critical heat flux is obtained by setting Peclet number equal to zero, which gives the minimum heat flux required to prevent the hot surface being rewetted. The numerical model is validated by comparing the results with known closed form solutions.*

Nomenclature

B = Biot number
C = specific heat
h = heat transfer coefficient
k = thermal conductivity
L = length of the tube
P_e = Peclet number
q = heat flux
Q = dimensionless heat flux
R, Z = dimensionless coordinates in quasi-steady state
r, z = physical coordinates
$\bar{r}, \bar{z}$ = coordinates in quasi-steady state
t = time
T = temperature
u = quench front velocity

Greek

α = stretching parameter
δ = radius ratio
θ = dimensionless temperature
ρ = density
ξ, η = coordinates after infinite-finite transformation

Subscripts

0 = quench front
1 = wet side
2 = dry side
s = saturation
w = wall condition

Introduction

The process of quenching of hot surfaces is of practical importance in the nuclear and metallurgical industries. For instance, in the event of a postulated loss-of-coolant accident (LOCA) in water cooled reactors, the clad surface of the fuel elements may reach a very high temperature because the stored energy in the fuel cannot be removed adequately by the surrounding steam. In order to bring the reactor to a cooled shutdown condition, an emergency core cooling system is activated to reflood the core. However, the injected coolant does not immediately wet the cladding surface because a stable vapor blanket will prevent the liquid-solid contact. Rewetting is the re-establishment of liquid contact with a hot solid surface whose initial temperature is higher than the

International Journal of Numerical Methods for Heat & Fluid Flow, Vol. 11 No. 3, 2001, pp. 200-212.
© MCB University Press, 0961-5539

The present investigation has been carried out with partial support from Grant No. F.8017/RDII/BOR/95, of AICTE, Government of India.

rewetting temperature, the maximal one for which the surface may wet. Surface rewetting is essential for effective heat removal. Also, the quenching phenomenon is of considerable practical interest in many other engineering applications, such as start-up of LNG pipe lines, filling of cryogenic vessels at room temperature, drying-out of evaporator tubes and heat treatment of various materials.

During the cooling process, a local wet patch is instantaneously formed, which eventually develops into a steadily moving quench front. As the quench front moves along the hot solid, two regions can be identified: a dry region ahead of the quench front and a wet region behind the quench front. In conduction-controlled rewetting analysis, it is believed that conduction of heat along the solid from dry region to wet region is the dominant mechanism of heat removal, which results in a lowering of the surface temperature immediately downstream of the quench front and causes the quench front to progress further. The upstream end of the solid is cooled by convection to the contacting liquid, while its downstream end is cooled by heat transfer to the mixture of vapor and entrained liquid droplets, called precursory cooling.

The two-dimensional rewetting model for two-region heat transfer with a step change in heat transfer coefficient at the quench front has been solved for a single slab (Olek, 1988) or for a composite slab (Olek, 1994). In the single slab model the dry region is considered to be adiabatic, whereas in the case of a composite slab a three-layer composite is considered to simulate the fuel and the cladding separated by a gas filled gap between them. Rewetting analyses in the cylindrical geometry have been carried out for a solid rod (Evans, 1984) or for a tube with an insulated core (Chakrabarti, 1986). The fuel-and-cladding model with adiabatic dry side has been solved in the composite axisymmetric geometry by Olek (1989). The rewetting model for a single slab geometry with boundary heat flux (to simulate the decay heating of the fuel) has been solved by Yao (1977). Chan and Zhang (1994) considered transient one-dimensional rewetting equation with a uniform heat flux in some other context, i.e. the design of heat pipes for thermal radiators. The solution methods commonly employed are either separation of variables or the Wiener-Hopf technique and solutions are obtained for either quench front temperature or quench front velocity.

In the present study, the physical model consists of an infinitely extended vertical tube with the outer surface flooded and the inner surface subjected to a uniform heat flux. The model assumes constant but different heat transfer coefficients for the wet and dry regions on the flooded side. The two-dimensional quasi-steady conduction equation governing the conduction-controlled rewetting has been solved by finite difference method. The main difficulty in the numerical solution of a rewetting problem is due to the infinite domain of the geometry and prescription of spatial boundary conditions at infinity. The pragmatic approach to achieve an approximate numerical solution of an infinite domain problem requires the far-field boundary to be fixed at a large but finite distance and the domain is only discretized up to this exterior

boundary. Such an attempt may require a large number of grid points and a rigorous experimentation. In the present paper an alternative method has been presented, in which the infinite physical domain is transformed to a finite computational domain. The value of the stretching parameter associated with the transformation has been found by minimizing the overall heat balance. The other difficulty lies in handling the mismatch boundary conditions at the quench front. Blair (1975) and Olek (1988) have observed that a jump in the boundary condition at the quench front yields a singularity in the analytical solutions. In the context of the present numerical treatment, the presence of this singularity may create an accuracy problem. This problem has been alleviated by imposing the continuity matching condition for both the temperature and the heat flux at the quench front, as described in the text. The present numerical solution involves the control volume discretization formulation with power law scheme and then solving the simultaneous algebraic equations by a block iterative method. The numerical model is validated by comparing the results with known analytical solutions.

Mathematical model

The two-dimensional transient heat conduction equation for the tube is

$$\frac{1}{r}\frac{\partial}{\partial r}\left(r\frac{\partial T}{\partial r}\right)+\frac{\partial^2 T}{\partial z^2}=\frac{\rho C}{k}\frac{\partial T}{\partial t} \quad r_1<r<r_2 \quad 0<z<L \quad L\to\infty \tag{1}$$

where L is the length of the tube and r_1 and r_2 are the inner and outer radius of the tube. The density, specific heat and thermal conductivity of the tube material are ρ, C and k respectively. The origin of the coordinate frame is at the bottom point on the axis of the tube. To convert this transient equation into a quasi-steady state equation, the following transformation is used:

$$\bar{r}=r \qquad \bar{z}=z-ut$$

where u is the constant quench front velocity and $\bar{r}$ and $\bar{z}$ are radial and axial coordinates respectively (Figure 1). Thus the transformed heat conduction equation in a coordinate system moving with the quench front is

$$\frac{1}{\bar{r}}\frac{\partial}{\partial \bar{r}}\left(\bar{r}\frac{\partial T}{\partial \bar{r}}\right)+\frac{\partial^2 T}{\partial \bar{z}^2}+\frac{\rho C u}{k}\frac{\partial T}{\partial \bar{z}}=0 \quad r_1<\bar{r}<r_2 \quad -\infty<\bar{z}<\infty \tag{2}$$

In conduction-controlled rewetting analysis the effect of coolant mass flux, coolant inlet subcooling and its pressure gradient etc. is not considered explicitly, but only implicitly in terms of wet region heat transfer coefficient, which is incorporated in the boundary condition. In the present study, the heat transfer coefficient h_1 is assumed to be constant over the entire wet region. The coolant temperature is taken to be equal to its saturation temperature T_s. On the dry side of the tube, the wall is cooled by the surrounding vapor. This cooling effect is very small compared with that of the wet region and is usually

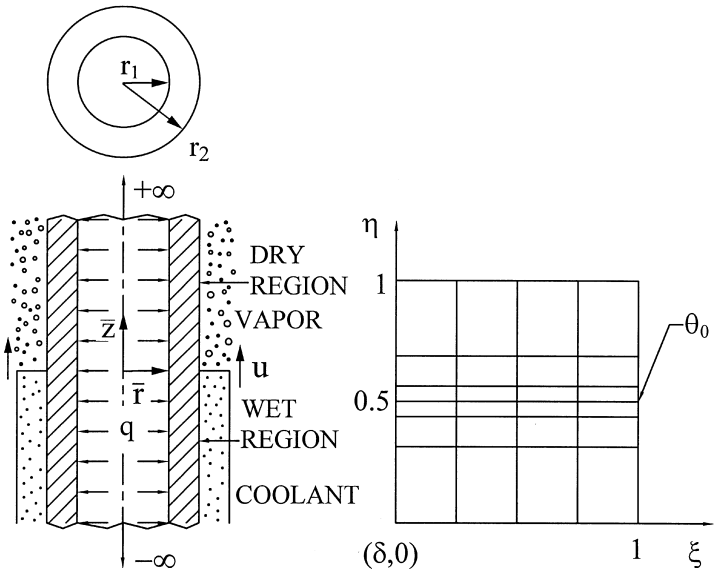

Figure 1.
Physical and computational domain of infinite tube

considered to be trivial in many rewetting models. However, this small cooling mechanism is very significant and essential in the rewetting analysis with boundary heat flux and cannot be neglected (Yao, 1977). The heat transfer coefficient accounting for both convective and radiative cooling effects on the dry side is assumed to be equal to h_2, a constant, which is smaller than h_1. The temperature of the surrounding vapor is assumed to beequal to T_w, which can be interpreted as the steady-state temperature of the hot surface prior to the onset of reflooding. Equation (2) can be expressed in the following dimensionless form:

$$\frac{1}{R}\frac{\partial}{\partial R}\left(R\frac{\partial\theta}{\partial R}\right)+\frac{\partial^2\theta}{\partial Z^2}+Pe\frac{\partial\theta}{\partial Z}=0 \qquad \delta<R<1 \qquad -\infty<Z<\infty \tag{3}$$

where δ is the radius ratio. The associated boundary conditions are:

$$\begin{array}{lll} \frac{\partial\theta}{\partial R}+Q=0 & \text{at} & R=\delta, \quad -\infty<Z<\infty \\ \frac{\partial\theta}{\partial R}+B_1\theta=0 & \text{at} & R=1, \quad Z<0 \\ \frac{\partial\theta}{\partial R}+B_2(\theta-1)=0 & \text{at} & R=1, \quad Z>0 \end{array} \tag{4}$$

The non-dimensional variables used above are:

$$\begin{array}{llll} R=\frac{\bar{r}}{r_2} & Z=\frac{\bar{z}}{r_2} & \theta=\frac{T-T_s}{T_w-T_s} & \delta=\frac{r_1}{r_2} \\ B_1=\frac{h_1 r_2}{k} & B_2=\frac{h_2 r_2}{k} & Pe=\frac{\rho C u r_2}{k} & Q=\frac{q r_2}{k(T_w-T_s)} \end{array} \tag{5}$$

The far-field boundary conditions may be derived with the assumption that the temperature field is sufficiently flat in the Z-direction at infinity

(Yao, 1977). Therefore, the first and second derivatives of temperature in Z-direction (i.e. $\partial\theta/\partial Z$ and $\partial^2\theta/\partial Z^2$) may be neglected at infinity ($Z \to \pm\infty$). With these two assumptions the far-field temperatures can be readily derived as:

$$\begin{aligned} \theta &= Q\delta\left(\tfrac{1}{B_1} - \ln R\right) && \text{at} && Z \to -\infty \\ \theta &= 1 + Q\delta\left(\tfrac{1}{B_2} - \ln R\right) && \text{at} && Z \to +\infty \end{aligned} \tag{6}$$

Estimation of rewetting (quench front) temperature is important in predicting the rate at which the coolant quenches the hot surface. The main objective of the present analysis is to obtain the temperature distribution in the domain for given values of wetside Biot number B_1, dryside Biot number B_2, Peclet number Pe and dimensionless heat flux Q. The non-dimensional quench front temperature is defined by:

$$\theta_0 = \frac{T_0 - T_s}{T_w - T_s} = \theta(1, 0) \tag{7}$$

where T_0 is the quench front temperature.

The infinite physical domain ($-\infty < Z < +\infty$) is then mapped to a finite computational domain (Figure 1) by the following infinite-finite transformation:

$$\xi = R \quad \text{and} \quad \eta = 0.5(1 + \tanh \alpha Z)$$

where α is the stretching parameter. The rationale of such a transformation is that the analytical boundary conditions at infinity can be implemented in the finite-difference equations. Although similar types of infinite-finite mapping functions (e.g. arctan or error function) do exist, the hyperbolic tangent is seemingly convenient to use, since the function is explicitly differentiable and invertible. The convection-diffusion equation (equation (3)) is thus transformed to:

$$\frac{\partial}{\partial\xi}\left(\frac{\xi}{\eta_z}\frac{\partial\theta}{\partial\xi}\right) + \frac{\partial}{\partial\eta}\left(\xi\eta_z\frac{\partial\theta}{\partial\eta} + \xi Pe\theta\right) = 0 \qquad \delta < \xi < 1 \qquad 0 < \eta < 1 \tag{8}$$

where $\eta_z = \frac{\partial\eta}{\partial Z} = 2\alpha\eta(1-\eta)$. The transformed boundary conditions are:

$$\begin{aligned} &\tfrac{\partial\theta}{\partial\xi} + Q = 0 && \text{at} && \xi = \delta, \ \ 0 < \eta < 1 \\ &\tfrac{\partial\theta}{\partial\xi} + B_1\theta = 0 && \text{at} && \xi = 1, \ \ \eta < 0.5 \\ &\tfrac{\partial\theta}{\partial\xi} + B_2(\theta - 1) = 0 && \text{at} && \xi = 1, \ \ \eta > 0.5 \\ &\theta = Q\delta\left(\tfrac{1}{B_1} - \ln\xi\right) && \text{at} && \eta = 0 \\ &\theta = 1 + Q\delta\left(\tfrac{1}{B_2} - \ln\xi\right) && \text{at} && \eta = 1 \\ &\theta = \theta_0 && \text{at} && \xi = 1, \ \ \eta = 0.5 \end{aligned} \tag{9}$$

Numerical solution

The five-point representation of the elliptic partial differential equation (equation (8)) can be written in the general form

$$A^0_{i,j}\theta_{i,j} = A^1_{i,j}\theta_{i,j+1} + A^2_{i,j}\theta_{i+1,j} + A^3_{i,j}\theta_{i,j-1} + A^4_{i,j}\theta_{i-1,j} + S_{i,j} \qquad (10)$$

The coefficients $A_{i,j}$ and the source term $S_{i,j}$ are evaluated by applying the power law scheme (Patankar, 1980) which makes use of integrating equation (8) over an elemental control volume, having a face area of $\Delta\xi\Delta\eta$. The same procedure is applicable to all the nodal points except at the quench front. In order to circumvent the discontinuous boundary conditions at the quench front, numerically, the coefficients of the discretized equation at this location have been obtained by an appropriate technique (Carnahan *et al.*, 1969). $\theta_{i,j}$ at the interface are expanded into Taylor series "forwards" for the dry region and "backwards" for the wet region, dropping terms beyond second order. These equations give $\left(\partial^2\theta/\partial\eta^2\right)_{i,j}$ for the dry and wet regions which, when substituted in the non-conservative form of equation (8), yield $(\partial\theta/\partial\eta)_{i,j}$ for the dry and wet regions, respectively. Now the expressions for $(\partial\theta/\partial\eta)_{i,j}$ at the interface are put in the following compatibility conditions to determine $A_{i,j}$ and $S_{i,j}$ of the discretized equation (10):

$$\left(\frac{\partial\theta}{\partial\eta}\right)^{I}_{i,j} = \left(\frac{\partial\theta}{\partial\eta}\right)^{\mathrm{II}}_{i,j} \quad \text{and} \quad \left(\theta\right)^{\mathrm{I}}_{\mathrm{i,j}} = (\theta)^{\mathrm{II}}_{\mathrm{i,j}}$$

where superscripts I and II denote dry and wet regions respectively. Expressions for the coefficients and the source term in equation (10) are tabulated in the Appendix. The simultaneous algebraic equations thus formed are then solved iteratively by "Strongly Implicit Procedure" (Stone, 1968). A convergence criterion of 0.01 percent change in θ at all the nodal points has been selected to test the convergence of the iterative scheme. All computations have been carried out using a non-uniform grid arrangement with 21 $\times$ 161 nodes. Since steep temperature gradients occur near the quench front, a grid structure has been adopted with finer grids near the quench front and progressively coarser grids away from it (Figure 1). Sample calculations were also carried out by doubling the grid size to ensure that the results are independent of the grid system. As is evident from the Appendix, the coefficients as well as the source term are independent of temperature and therefore they do not pose any divergence problem.

To further check the accuracy of the numerical results, the overall heat balance criterion is verified. By integrating equation (8) over the entire computational domain, the heat balance equation can be derived as:

$$\frac{Pe(1-\delta^2)}{2}\left(1+\frac{Q\delta}{B_2}-\frac{Q\delta}{B_1}\right) = \int_0^{0.5}\frac{B_1\theta|_{\xi=1}-Q\delta}{2\alpha\eta(1-\eta)}d\eta + \int_{0.5}^{1.0}\frac{B_2(\theta|_{\xi=1}-1)-Q\delta}{2\alpha\eta(1-\eta)}d\eta \qquad (11)$$

The integrals of equation (11) have been evaluated by Simpson's 1/3 rule. It may be noted that, as the first and second integral of equation (11) become improper at $\eta = 0$ and at $\eta = 1$ respectively, the indeterminate form of the integrals at these locations is overcome by applying L'Hôpital rule. The absolute difference between the right and left sides of the above equation is first divided by the minimum of the two values and then multiplied by 100 to get the percentage difference.

The heat balance equation (equation (11)) indicates the fact that, with particular choice of α, it is possible to satisfy the heat balance. In this respect, if the heat balance difference so obtained is assumed to be the objective function, the stretching parameter used in the mapping function can be treated as an independent variable. Thus, starting from an arbitrary base point ($\alpha > 0$), the variable can be moved towards an optimum based on sequential minimization of the objective function. To reduce the number of function evaluations, an optimization technique (Golden Section Search) is used that does not require the derivative of the function. A tolerance limit of 0.01 percent change of the function value has been selected, below which the search process is terminated. The heat balance, achieved through minimization as above, establishes the accuracy of the temperature field obtained and thereby determines the optimal value of the stretching parameter.

Results and discussion

The numerical computation of the temperature field has been carried out with B_1, B_2, Pe, Q and δ as input parameters. In particular, the variation of quench front temperature with respect to the above model parameters is shown in the graphical form. Temperature estimates are also obtained for the limiting case of a solid rod where the radius ratio as well as the heat flux are taken as zero. Reported literature on experimental investigation on quenching (Barnea *et al.*, 1994) indicates that quench front exists in the transition boiling zone. The heat transfer coefficient in the transition zone is estimated to be 10^5~10^6W/m^2 – K and the vapor cooling heat transfer coefficient in the film boiling zone is in the order of 10^2 W/m^2 – K. Therefore, in the present analysis the values of B_2 are set equal to $10^{-3}B_1$.

The temperature profiles for the outer surface of the tube are illustrated in Figure 2 for different Peclet numbers with $Q = 0.01$ and $B_1 = 10$. The temperature at $\eta = 1$ is $Q\delta/B_2$ higher than the initial wall temperature. Similarly, the temperature at $\eta = 0$ is $Q\delta/B_1$ higher than the coolant temperature. At lower values of Peclet number (for $Pe = 0.1$ and 1.0), a part of the dry region immediately ahead of the quench front has a temperature less than 1 and the other part is more than 1. This implies that the former part of the dry region will be heated by the vapor instead of being cooled, as the temperature of the vapor is assumed to be equal to the initial wall temperature. But in the case of higher Peclet numbers (for $Pe = 10$ and 100), the whole of the dry region is of a temperature greater than 1 and it will be cooled by vapor. Moreover, quench front temperature is found to increase with increase in Peclet number. With fixed

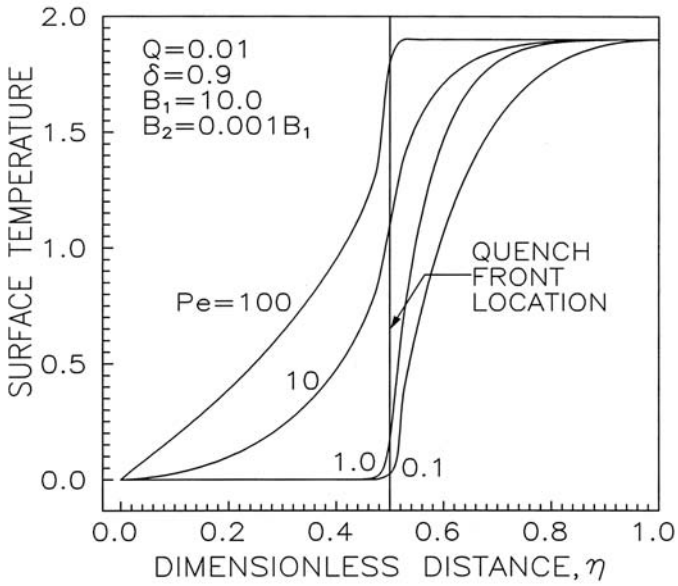

Figure 2. Surface temperature distribution on the coolant side for various Peclet numbers

material properties and dimensions, Peclet number and Biot number represent the quench front velocity and the heat transfer coefficient respectively. For the specified heat flux and Biot numbers, the quench front temperature increases with the increase in quench front velocity. This is probably due to the fact that a higher relative velocity between the tube and the coolant allows less time for sufficient heat transfer to take place, resulting in a higher value of θ_0. The above trend also reflects the fact that, for the same rewetting rate, an increasing cladding thermal diffusivity tends to reduce θ_0.

The temperature profiles for the outer surface of the tube for different Biot numbers are shown in Figure 3. In this case, quench front temperature decreases with the increase in Biot number for a given *Pe, Q* and δ. A higher Biot number results in a higher heat transfer coefficient, which may cause a decrease in θ_0. The temperature gradient at the quench front also increases with the increase in Biot number in the computational domain. This reveals the fact, that at higher values of heat transfer coefficients, the axial conduction across the quench front may be significant.

The dependence of the quench front temperature on Biot number and dimensionless heat flux is shown in Figure 4. For a fixed Biot number, the quench front temperature increases with the increase in *Q*. Apparently, a higher heat flux causes more heat transfer to the cladding and hence this would increase θ_0. Also, in this case the quench front temperature decreases with increase in Biot number, consistent with Figure 3. The above trends are in obvious accord with the interpretations based on physical ground. In all cases, θ_0 decreases as the Biot number increases, reflecting the fact that a quench front progresses more easily when the heat transfer to the coolant is increased. Figure 5 shows the

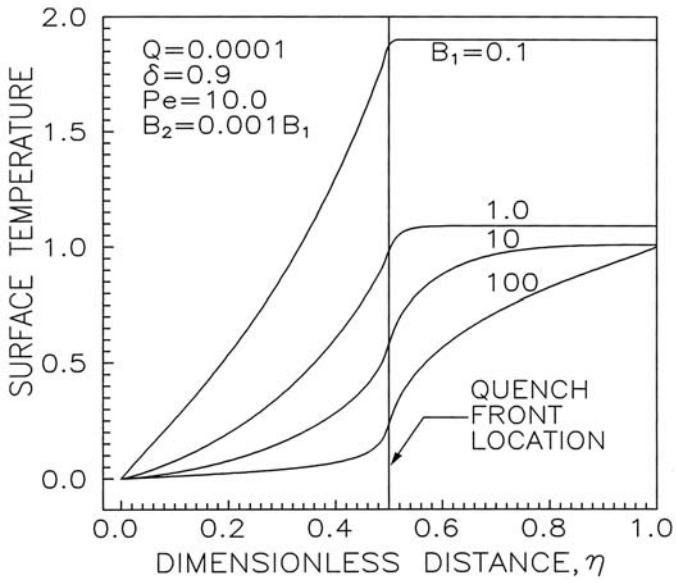

Figure 3.
Surface temperature distribution on the coolant side for various Biot numbers

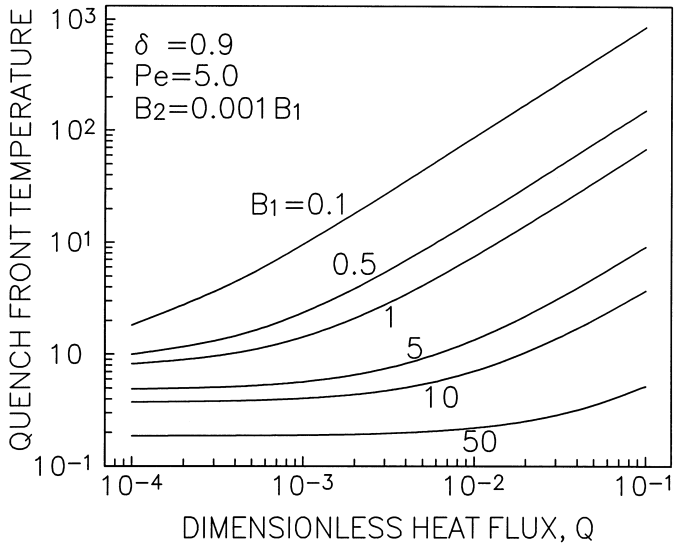

Figure 4.
Quench front temperature for various heat flux and Biot numbers

effect of radius ratio δ on quench front temperature for the fixed values of B_1, Pe and Q. Although θ_0 increases with increase in δ in the presence of boundary heat flux, an opposite trend is observed in the case of zero heat flux.

The variation of θ_0 on Biot number and Q for the case of zero Peclet number has been displayed in Figure 6. The physical meaning of $Pe = 0$ is that the quench front ceases to move when Q approaches its critical value. In such cases, the tube can no longer be wetted. For $Q > Q_{cri}$, the quench front will

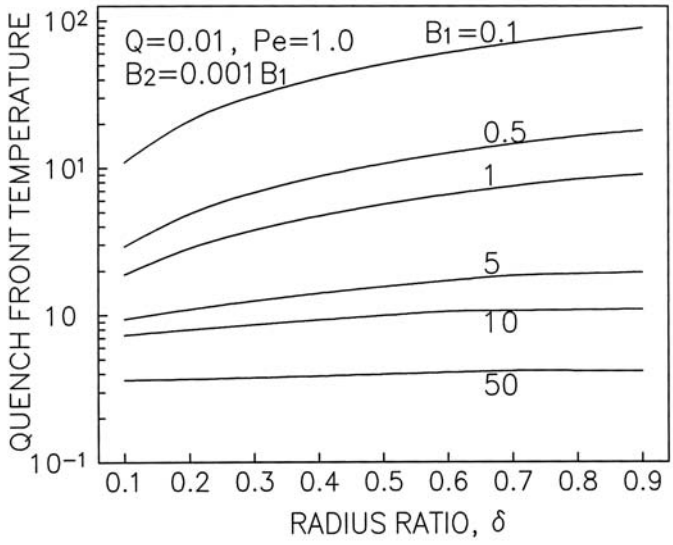

Figure 5.
Quench front temperature variation with radius ratio and Biot number

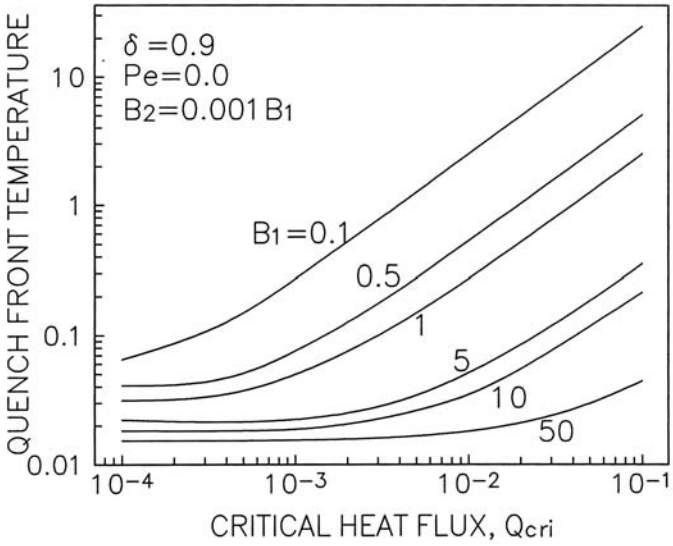

Figure 6.
Quench front temperature at the critical heat flux

reverse its direction and the wetted surface will be dried. In this case, the tube will be heated by a heat flux that exceeds the maximum heat removal capacity by convection and boiling. Thus dryout will occur.

Finally, the model is reduced to that of the conventional model (tube with insulated inner core and no precursory cooling). By setting $Q = 0$, the present model simulates the flooding situation of a hot tube with an inside adiabatic surface and without any precursory cooling. The present solution also reduces to

that of a solid cylinder by setting $\delta = 0$ and $Q = 0$. The present solution has been compared with those of Olek (1989) in Figures 7 and 8. As expected, the quench front temperature increases with the increase in Peclet number and with the decrease in Biot number. The numerical results are in good agreement with the analytical ones for low Biot numbers, while the accuracy deteriorates as the Biot number becomes large. This is probably due to the existence of mismatch boundary conditions (normal temperature gradient i.e. $\partial\theta/\partial\xi$) at the quench front (equation (9)). Apparently, the strength of the discontinuity increases with

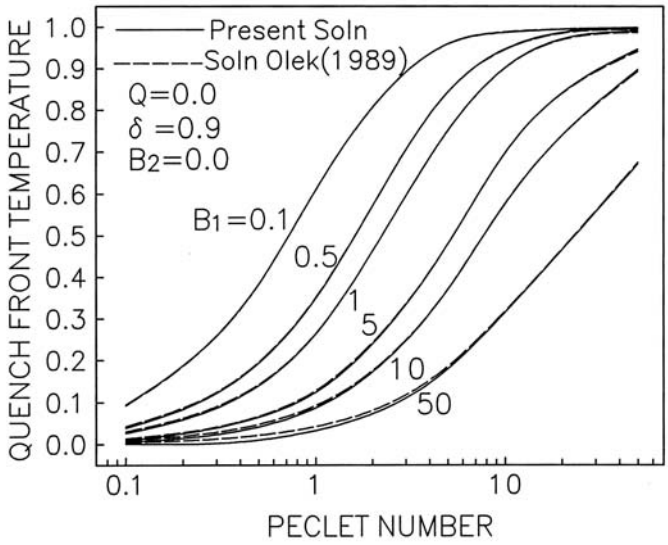

Figure 7.
Quench front temperature variation with Biot and Peclet number for the tube with $\delta = 0.9$

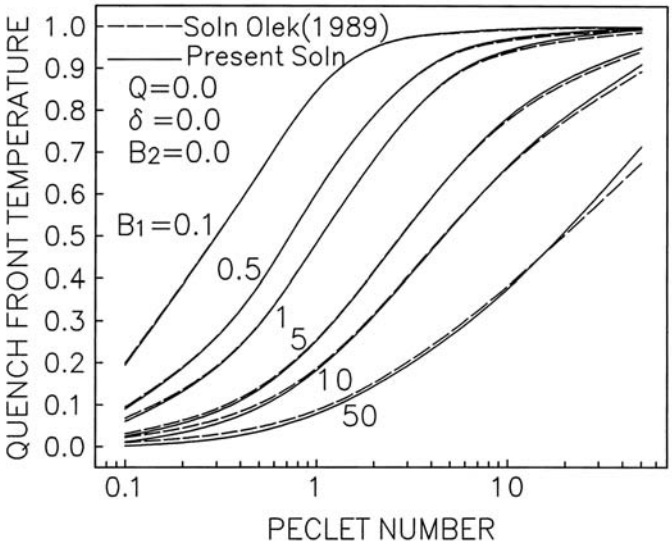

Figure 8.
Quench front temperature variation with Biot and Peclet number for the rod ($\delta = 0$)

the increase in Biot number and, thus, the accuracy of the solution deteriorates. On the contrary, the Wiener-Hopf solution has been proved to be the most accurate one in handling discontinuous boundary conditions, which makes use of decomposing an appropriate kernel function in the complex Fourier domain. Nevertheless, the present solution may be beneficial in the case of solving non-linear rewetting equations arising due to temperature dependent thermo-physical properties, whereas a plausible analytical solution may not exist.

Conclusion

A numerical solution for solving infinite domain problems arising out of rewetting analysis has been suggested. The value of stretching parameter used for infinite-finite transformation can be obtained by minimizing the heat balance. In general, quench front temperature is found to increase with the increase in Peclet number and dimensionless heat flux, and with the decrease in Biot number. The boundary conditions in the present formulation require liquid/vapor temperatures and liquid/vapor heat transfer coefficients as input parameters, these limitations being inherent in a conduction-controlled rewetting model. The arbitrariness of the choice of their values can only be eliminated if a conjugate heat transfer model is considered. The present numerical procedure may therefore be extended to the conjugate heat transfer problem, where the energy equations of solid, liquid and vapor regions need to be solved simultaneously.

References

Barnea, Y., Elias, E. and Shai, I. (1994), "Flow and heat transfer regimes during quenching of hot surfaces", *International Journal of Heat and Mass Transfer*, Vol. 37, pp. 1441-53.

Blair, J.B. (1975), "An analytical solution to a two-dimensional model of the rewetting of a hot dry rod", *Nuclear Engineering and Design*, Vol. 32, pp. 159-70.

Carnahan, B., Luther, H.A. and Wilkes, J.O. (1969), *Applied Numerical Methods*, John Wiley & Sons, New York, NY, p. 462.

Chakrabarti, A. (1986), "The sputtering temperature of a cooling cylindrical rod with an insulated core", *Applied Scientific Research*, Vol. 43, pp. 107-13.

Chan, S.H. and Zhang, W. (1994), "Rewetting theory and the dryout heat flux of smooth and grooved plates with a uniform heating", *ASME Journal of Heat Transfer*, Vol. 116, pp. 173-9.

Evans, D.V. (1984), "A note on the cooling of a cylinder entering a fluid", *IMA Journal of Applied Mathematics*, Vol. 33, pp. 49-54.

Olek, S. (1988), "On the two-region rewetting model with a step change in the heat transfer coefficient", *Nuclear Engineering and Design*, Vol. 108, pp. 315-22.

Olek, S. (1989), "Solution to a fuel-and-cladding rewetting model", *International Communications in Heat and Mass Transfer*, Vol. 16, pp. 146-58.

Olek, S. (1994), "Quenching of a composite slab", *International Communications in Heat and Mass Transfer*, Vol. 21, pp. 333-44.

Patankar, S.V. (1980), *Numerical Heat Transfer and Fluid Flow*, Hemisphere, Washington, DC, p. 96.

Stone, H.L. (1968), "Iterative solution of implicit approximations of multidimensional partial differential equations", *SIAM Journal of Numerical Analysis*, Vol. 5, pp. 530-58.

Yao, L.S. (1977), "Rewetting of a vertical surface with internal heat generation", *AIChE Symposium Series*, Vol. 73, pp. 46-50.

Appendix. Coefficients of finite difference equations

(a) Internal and boundary nodes (except at the quench front):

$$A^1_{i,j} = f(\xi)\frac{\eta^+_z}{h_2}\left\| 0 \quad , \quad \left(1 - \frac{0.1Peh_2}{\eta^+_z}\right)^5 \right\| + f(\xi).Pe \qquad , \qquad A^2_{i,j} = \frac{2f_1 I(\eta)}{h_1}$$

$$A^3_{i,j} = f(\xi)\frac{\eta^-_z}{h_4}\left\| 0 \quad , \quad \left(1 - \frac{0.1Peh_4}{\eta^-_z}\right)^5 \right\| \qquad , \qquad A^4_{i,j} = \frac{2f_2 I(\eta)}{h_3}$$

$$A^0_{i,j} = \sum_{k=1}^{4} A^k_{i,j} + 2f_3 I(\eta) \qquad , \qquad S_{i,j} = 2f_4 I(\eta)$$

For internal nodes: $f_1 = \xi^+/(h_1 + h_3) \quad f_2 = \xi^-/(h_1 + h_3) \quad f_3 = f_4 = 0 \quad f(\xi) = (\xi^+ + \xi^-)/2$

For boundary nodes: $(\xi = \delta)$: $f_1 = \xi^+/h_1 \quad f_2 = f_3 = 0 \quad f_4 = Q\delta/h_1 \quad f(\xi) = (\delta + \xi^+)/2$

$(\xi = 1, \eta > 0.5)$: $f_1 = 0 \quad f_2 = \xi^-/h_3 \quad f_3 = f_4 = B_2/h_3 \quad f(\xi) = (1 + \xi^-)/2$

$(\xi = 1, \eta < 0.5)$: $f_1 = f_4 = 0 \quad f_2 = \xi^-/h_3 \quad f_3 = B_1/h_3 \quad f(\xi) = (1 + \xi^-)/2$

(b) Quench front node: (ξ = 1, η = 0.5)

$$A^1_{i,j} = \frac{1}{2}\left(Pe + \frac{\alpha}{h_2}\right)\left(Pe + \frac{\alpha}{h_4}\right) \qquad A^2_{i,j} = 0 \qquad A^3_{i,j} = \frac{1}{2}\left(\frac{\alpha}{h_4}\right)^2 \qquad A^4_{i,j} = \frac{2}{h_3^2}\left(1 + \frac{h_2}{h_4} + \frac{Peh_2}{\alpha}\right)$$

$$A^0_{i,j} = \sum_{k=1}^{4} A^k_{i,j} + \left(1 + \frac{2}{h_3}\right)\left[B_1 + B_2\left(\frac{h_2}{h_4} + \frac{Peh_2}{\alpha}\right)\right] \qquad S_{i,j} = B_2\left(1 + \frac{2}{h_3}\right)\left(\frac{h_2}{h_4} + \frac{Peh_2}{\alpha}\right)$$

where $I(\eta) = \dfrac{1}{2\alpha}\ln\left[\dfrac{\eta^+}{\eta^-}\dfrac{1-\eta^-}{1-\eta^+}\right] \quad , \quad \eta_z = 2\alpha\eta(1-\eta)$

$h_1 = \xi_{i+1} - \xi_i, \qquad h_2 = \eta_{j+1} - \eta_j, \qquad h_3 = \xi_i - \xi_{i-1}, \qquad h_4 = \eta_j - \eta_{j-1}$

Superscripts plus and minus in ξ denote $(i + 1/2, j)$ and $(i - 1/2, j)$ locations.

Superscripts plus and minus in η denote $(i, j + 1/2)$ and $(i, j - 1/2)$ locations.

$\| \ \|$ denotes larger between the two values.